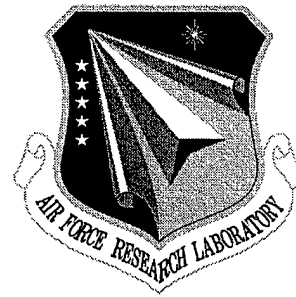


**AFRL-IF-RS-TM-2000-1**  
**In-House Technical Memorandum**  
**July 2000**



# **AN INTRODUCTION TO A FEEDFORWARD DEMODULATOR**

**Andrew J. Noga**

*APPROVED FOR PUBLIC RELEASE; DISTRIBUTION UNLIMITED.*

**AIR FORCE RESEARCH LABORATORY  
INFORMATION DIRECTORATE  
ROME RESEARCH SITE  
ROME, NEW YORK**

**DIC QUALITY INSPECTED \***

**20000802 231**

This report has been reviewed by the Air Force Research Laboratory, Information Directorate, Public Affairs Office (IFOIPA) and is releasable to the National Technical Information Service (NTIS). At NTIS it will be releasable to the general public, including foreign nations.

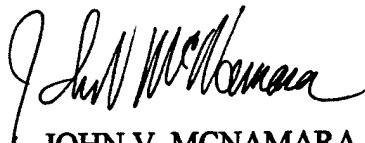
AFRL-IF-RS-TM-2000-1 has been reviewed and is approved for publication.

APPROVED:



GERALD C. NETHERCOTT  
Chief, Multi-Sensor Exploitation Branch  
Info and Intel Exploitation Division  
Information Directorate

FOR THE DIRECTOR:



JOHN V. MCNAMARA, Technical Advisor  
Info and Intel Exploitation Division  
Information Directorate

If your address has changed or if you wish to be removed from the Air Force Research Laboratory Rome Research Site mailing list, or if the addressee is no longer employed by your organization, please notify AFRL/IFEC, 32 Brooks Road, Rome, NY 13441-4114. This will assist us in maintaining a current mailing list.

Do not return copies of this report unless contractual obligations or notices on a specific document require that it be returned.

REPORT DOCUMENTATION PAGE			Form Approved OMB No. 0704-0188	
Public reporting burden for this collection of information is estimated to average 1 hour per response, including the time for reviewing instructions, searching existing data sources, gathering and maintaining the data needed, and completing and reviewing the collection of information. Send comments regarding this burden estimate or any other aspect of this collection of information, including suggestions for reducing this burden, to Washington Headquarters Services, Directorate for Information Operations and Reports, 1215 Jefferson Davis Highway, Suite 1204, Arlington, VA 22202-4302, and to the Office of Management and Budget, Paperwork Reduction Project (0704-0188), Washington, DC 20503.				
1. AGENCY USE ONLY (Leave blank)	2. REPORT DATE July 2000	3. REPORT TYPE AND DATES COVERED In House, November 1998 - November 1999		
4. TITLE AND SUBTITLE AN INTRODUCTION TO A FEEDFORWARD DEMODULATOR		5. FUNDING NUMBERS C: N/A PE: 62702F PR: 459E		
6. AUTHOR(S) Dr. Andrew J. Noga				
7. PERFORMING ORGANIZATION NAME(S) AND ADDRESS(ES) AFRL/IFEC 32 Brooks Road Rome NY 13441-4114		8. PERFORMING ORGANIZATION REPORT NUMBER  AFRL-IF-RS-TM-2000-1		
9. SPONSORING/MONITORING AGENCY NAME(S) AND ADDRESS(ES) AFRL/IFEC 32 Brooks Road Rome NY 13441-4114		10. SPONSORING/MONITORING AGENCY REPORT NUMBER  AFRL-IF-RS-TM-2000-1		
11. SUPPLEMENTARY NOTES  Air Force Research Laboratory Project Engineer: Dr. Andrew Noga/IFEC/315-330-2270				
12a. DISTRIBUTION AVAILABILITY STATEMENT  Approved for public release; distribution unlimited		12b. DISTRIBUTION CODE		
13. ABSTRACT (Maximum 200 words) An introduction is given to the Reconstituted FM with Feedforward (RFF) demodulator, U.S. Patent 6,002,298. This report provides the necessary background and motivation for conducting further research regarding the performance and application of this angle-demodulation technique. A comparison is made between this new technique and a standard method of angle-demodulation by simulating a specific input signal scenario. Areas requiring further research are cited.				
14. SUBJECT TERMS Angle-demodulation, demodulation, feedforward, reconstitution			15. NUMBER OF PAGES 32	
			16. PRICE CODE	
17. SECURITY CLASSIFICATION OF REPORT  UNCLAS	18. SECURITY CLASSIFICATION OF THIS PAGE  UNCLAS	19. SECURITY CLASSIFICATION OF ABSTRACT  UNCLAS	20. LIMITATION OF ABSTRACT  UL	

## TABLE OF CONTENTS

<b>Executive Summary</b>	<b>ii</b>
<b>1 Overview of Angle-Demodulation and the RFF Demodulator</b>	<b>1</b>
1.1 Angle-Demodulation Background	1
1.1.1 Non-coherent Angle-Demodulation	2
1.1.2 Limitations and Disadvantages of Non-coherent Angle-Demodulation	8
1.1.3 Coherent Angle-Demodulation	10
1.1.4 Limitations and Disadvantages of Coherent Angle-Demodulation	12
1.2 Standard Non-coherent Angle-Demodulation Results	13
<b>2 RFF Background</b>	<b>15</b>
2.1 Description, Manner and Process of Using the RFF Demodulator	16
2.1.1 Alternative RFF Configurations	19
2.1.2 RFF Advantages	20
2.2 Demodulation Results Using the RFF	21
<b>3 Summary</b>	<b>23</b>
<b>4 References</b>	<b>24</b>

## **Executive Summary**

This technical memorandum represents an initial report on the patented Reconstituted FM with Feedforward demodulator, which has been developed at the Air Force Research Laboratory (AFRL). The intent of this report is to provide the necessary background and motivation for conducting further research regarding the performance and application of this demodulation technique. A comparison is made between this new technique and a standard method of angle modulation recovery by simulating a specific input signal scenario. The scenario is that of a frequency-chirped pulsed-carrier, as presented in the associated patent. Areas requiring further research are cited in the summary section. The work has been supported by both the Air Force Office of Scientific Research (AFOSR) Entrepreneurial Research (ER) program, and by the Information Directorate of the AFRL.

## 1 Overview of Angle-Demodulation and the RFF Demodulator

The purpose of the Reconstituted FM with Feedforward (abbreviated R-FMFF, or simply RFF) demodulator (U.S. Patent No. 6,002,298) is to obtain an enhanced estimate of the angle-modulation,  $\phi(t)$ , imposed on a transmitted Radio Frequency (RF) or Intermediate Frequency (IF) carrier. In particular, there is an “ideal” receiver bandwidth and center frequency that can be determined, based on the trade-off of the effects of additive noise (and interference) with the effects of distortions due to non-ideal transfer function characteristics. Having too large a bandwidth results in an unnecessary amount of additive noise. Having too narrow a bandwidth makes the system sensitive to center frequency tuning, and can lead to gain and phase related signal distortions. Where possible, selection and use of an ideal receiver bandwidth and center frequency, will jointly minimize noise and receiver-induced distortions onto the received signal, thereby maintaining a higher fidelity in the recovered angle-modulation. The intent of the RFF demodulator is to allow for the use of a narrower band-pass filter to reject noise, while simultaneously reducing transfer-function-induced signal distortions and maintaining center frequency tuning. As will be demonstrated the RFF demodulator can provide more robust angle-modulation estimation when a-priori knowledge is limited.

### 1.1 Angle-Demodulation Background

General reference is made to [1] for additional detail and further references on angle-modulation and demodulation systems. A concise summary of both non-coherent and coherent angle-demodulation methods is provided for background purposes.

### 1.1.1 Non-coherent Angle-Demodulation

The typical non-coherent angle-modulation recovery or estimation process consists of a Band-pass Filter, a Phase Differentiator and a Low-pass Filter-Integrator as shown in Figure 1-1. The function of the Band-pass Filter is to pre-condition the IF input signal, by allowing the frequency band occupied by the desired signal,  $s(t)$ , to pass through, while rejecting all other frequencies. However, since some of the noise,  $W(t)$ , occupies the same frequency band as  $s(t)$ , the Band-Pass Filter passes both the desired signal,  $s(t)$ , and the noise constituent,  $N(t)$ . The output of the Band-pass Filter can be modeled as

$$X(t) = \{s(t)\}_{BPF} + N(t), \quad (1.1)$$

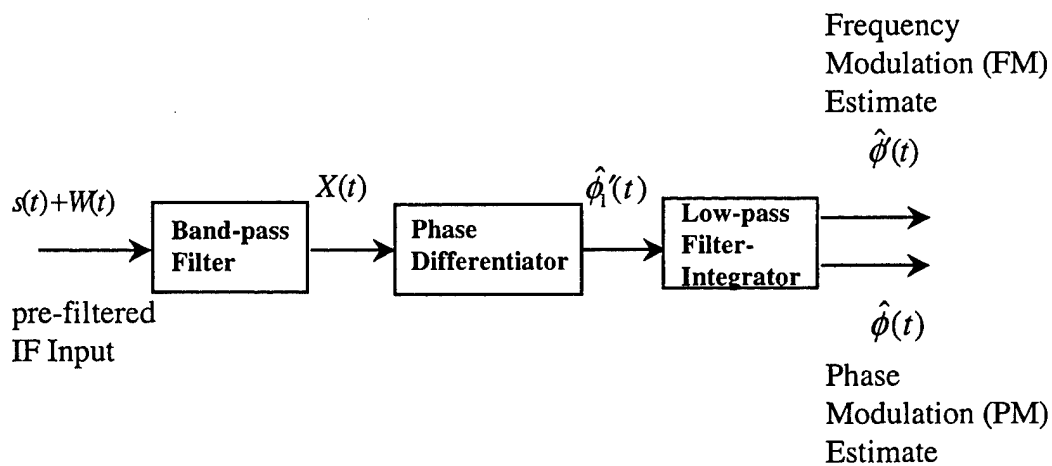


Figure 1-1. Typical angle-modulation estimation process.

where the notation  $\{\cdot\}_{BPF}$  represents the effects of the Band-pass Filter, and where  $N(t) = \{W(t)\}_{BPF}$ . This filtered IF signal,  $X(t)$ , is then input to some form of a Phase Differentiator resulting in  $\hat{\phi}'_1(t)$ , as shown in the figure. Many techniques exist and are described in the literature for performing this function. Included among these techniques for example are zero crossing measurement (which is inversely proportional to signal frequency), and frequency-to-voltage conversion with envelope detection (often referred to as an FM discriminator). A mathematical model for the Phase Differentiator process will be developed in following paragraphs. At this point it is sufficient to describe this process as a measurement of the rate-of-change of phase of a signal, with respect to time. Finally, this time rate-of-change of phase is processed by a Low-pass Filter which has a cut-off frequency commensurate with the bandwidth of the original message or information signal,  $m(t)$ . Depending on the type of angle modulation used, frequency modulation or phase modulation, either  $\hat{\phi}'(t)$ , the low-pass filtered time rate-of-change of phase measurement, or the integral,  $\hat{\phi}(t) = \int_0^t \hat{\phi}'(\tau) d\tau$ , will be of interest. For frequency modulation,  $\phi(t)$  is generated at the transmitter source as

$$\phi(t) = 2\pi \cdot \Delta f \int_0^t m_{FM}(\tau) d\tau, \quad (1.2)$$

in which case, the output  $\hat{\phi}'(t) \equiv 2\pi \cdot \Delta f \cdot m_{FM}(t)$  is of interest since this signal is proportional to the original message,  $m_{FM}(t)$ . Generally, the message signal,



$m(t) = m_{FM}(t)$  or  $m(t) = m_{PM}(t)$ , is modeled as being normalized such that  $-1 \leq m(t) \leq +1$ , and the factor  $\Delta f$  controls the frequency deviation of  $s(t)$ . Likewise for phase modulation,  $\phi(t)$  is generated at the transmitter source as

$$\phi(t) = k_p \cdot m_{PM}(t), \quad (1.3)$$

in which case the output  $\hat{\phi}(t) \equiv k_p \cdot m_{PM}(t)$  is of interest. Here,  $k_p$  is some proportionality scale factor. (More sophisticated angle-modulation systems may employ pre-emphasis/de-emphasis filters which operate on the message signal and the estimated message respectively, to help offset the adverse effects of noise. However, without loss of generality, these filters can be modeled as being incorporated into our message signal and Low-pass Filter / Integrator processes.)

A sufficient condition for us to be able to properly employ analytic signal representation [1] in any practical system, is that the signal being processed be a band-pass signal. Using this fact, an equivalent model of the Phase Differentiator process is shown in Figure 1-2. The function of the Analytic Signal Extractor is to generate the analytic signal,  $X_+(t)$ . This signal contains both the imposed angle modulation which is of interest plus phase distortion and can be represented as

$$X_+(t) = |A(t)| \exp\{j \cdot [2\pi f_c t + \phi(t) + \eta(t) - \theta]\}. \quad (1.4)$$

Here,  $|A(t)| > 0$ , is the envelope of  $X_+(t)$ , and  $\theta$  is some constant phase offset. The term  $f_c$  represents the center frequency which is assumed to be known within some small tuning error.

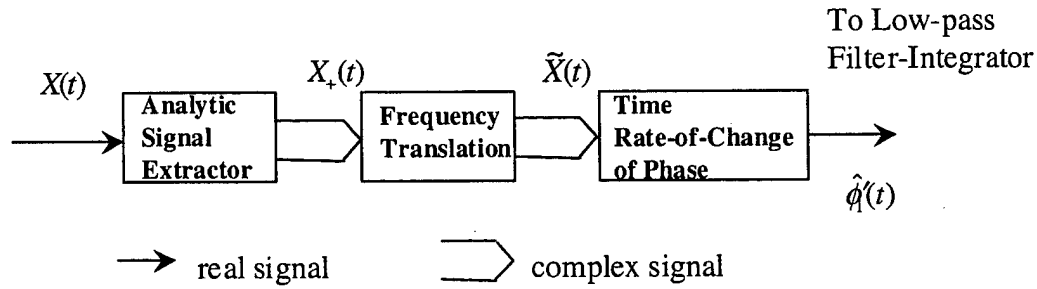


Figure 1-2. Equivalent analytic representation of the Phase Differentiator.

The term  $\eta(t)$  represents some phase angle distortion due to the imperfect receive channel. Following the Analytic Signal Extractor, a Frequency Translation process is performed. This process simply consists of the complex multiplication of the input,  $X_+(t)$ , with the complex exponential

$$z_-(t) = \exp\{-j \cdot 2\pi \hat{f}_c t\}, \quad (1.5)$$

where  $\hat{f}_c$  is the known constituent of the center frequency. This complex product produces what can be referred to as the *complex envelope* of  $X(t)$ . By employing analytic signal notation, we can represent the input signal in complex envelope form as

$$\tilde{X}(t) = |A(t)| \exp\{j \cdot [2\pi f_e t + \phi(t) + \eta(t) - \theta]\}, \quad (1.6)$$

where  $f_e = f_c - \hat{f}_c$  is some small tuning frequency error. Alternatively,  $\tilde{X}(t)$  can be represented in rectangular form as

$$\tilde{X}(t) = X_i(t) + jX_q(t), \quad (1.7)$$

where  $X_i(t) = |A(t)| \cos[2\pi f_e t + \phi(t) + \eta(t) - \theta]$  is the real component of  $\tilde{X}(t)$ , and  $X_q(t) = |A(t)| \sin[2\pi f_e t + \phi(t) + \eta(t) - \theta]$  is the imaginary component of  $\tilde{X}(t)$ . It can be shown that the time rate-of-change of phase of the complex signal  $\tilde{X}(t)$  is

$$\begin{aligned} \hat{\phi}_1'(t) &= \frac{d}{dt} \left\{ \tan^{-1} \left[ \frac{X_q(t)}{X_i(t)} \right] \right\} \\ &= \frac{X_i(t) \frac{d}{dt} \{X_q(t)\} - X_q(t) \frac{d}{dt} \{X_i(t)\}}{X_i^2(t) + X_q^2(t)}, \quad -\frac{\pi}{2} < \tan^{-1} \left\{ \frac{X_q(t)}{X_i(t)} \right\} < \frac{\pi}{2}. \end{aligned} \quad (1.8)$$

From the above, we find that the rate-of-change of phase of  $\tilde{X}(t)$  is

$$\hat{\phi}_1'(t) = 2\pi f_e + \phi'(t) + \eta'(t) \quad (\text{radians per second}). \quad (1.9)$$

This estimate contains the bias term,  $2\pi f_e$ , and an error term,  $\eta'(t)$ , and can easily be converted to units of Hz, by scaling by the factor  $1/2\pi$ . We find that for frequency modulation, with the Low-pass Filtering process indicated as  $\{\cdot\}_{LPF}$ ,

$$\hat{\phi}'(t) = \left\{ \hat{\phi}'_1(t) \right\}_{LPF} = \left\{ 2\pi f_e + 2\pi \Delta f \cdot m_{FM}(t) + \eta'(t) \right\}_{LPF}. \quad (1.10)$$

For phase modulation,

$$\hat{\phi}(t) = \left\{ 2\pi f_e t + k_p \cdot m_{PM}(t) + \eta(t) + \theta_c \right\}_{LPF}, \quad (1.11)$$

where  $\theta_c$  is some initial-condition dependent constant phase offset. (Note that  $m_{FM}(t)$

and  $m_{PM}(t)$  are related as  $k_p \cdot m_{PM}(t) = 2\pi \Delta f \int_0^t m_{FM}(\tau) d\tau$ .)

This summarizes the non-coherent method of angle-demodulation; many implementation variations of the method exist, however, each can be similarly modeled as above. Note that this includes those non-coherent angle-demodulation techniques which perform some type of “hard limiting” or normalization on the envelope of  $X(t)$  prior to angle-modulation recovery. This is made evident by the normalization factor  $1/\left(X_i^2(t) + X_q^2(t)\right)$  employed in the phase differentiation process. The purpose of normalization is to de-sensitize the phase angle measurement to variations in envelope, thus reducing the phase distortion component,  $\eta(t)$ .

### 1.1.2 Limitations and Disadvantages of Non-coherent Angle-Demodulation

The previous development exposes the limitations of the non-coherent method of angle-demodulation. This method does not take advantage of the fact that the message signal,  $m(t)$ , and therefore the modulated signal,

$$s_+(t) = |a(t)| \exp\{j \cdot [2\pi f_c t + \phi(t) - \theta]\}, \quad (1.12)$$

can be highly correlated at consecutive time instants. (Here,  $|a(t)| > 0$  is some slowly changing or constant envelope that is present on the transmitted signal.) More specifically, the spectral content of  $m_{FM}(t)$  is essentially limited to some maximum frequency,  $f_m$  Hz, therefore when the deviation ratio

$$\beta = \frac{\Delta f}{f_m} \quad (1.13)$$

is large (i.e., is greater than 10), it is possible to employ some form of adaptive band-pass filtering prior to rate-of-change of phase measurement. By doing so, the bandwidth of the band-pass filter process can be made more narrow, thus rejecting more of the additive (analytic) noise,  $W_+(t)$ .

An additional related disadvantage of the non-coherent method of angle-demodulation arises due to the tuning error,  $f_e$ . This tuning offset can lead to an increase in the phase distortion term,  $\eta(t)$ , since the Band-pass Filter process shown in Figure 1-1

is designed to operate at the center frequency,  $f_c$ . The resulting off-centering of the input signal causes a distortion of the desired signal, such that  $\{s(t)\}_{BPF} \neq s(t)$ . In particular, the band-pass filter will have undesired attenuation and phase changes near the band edges which adversely affect the overall angle-demodulation process. This problem is depicted in Figure 1-3.

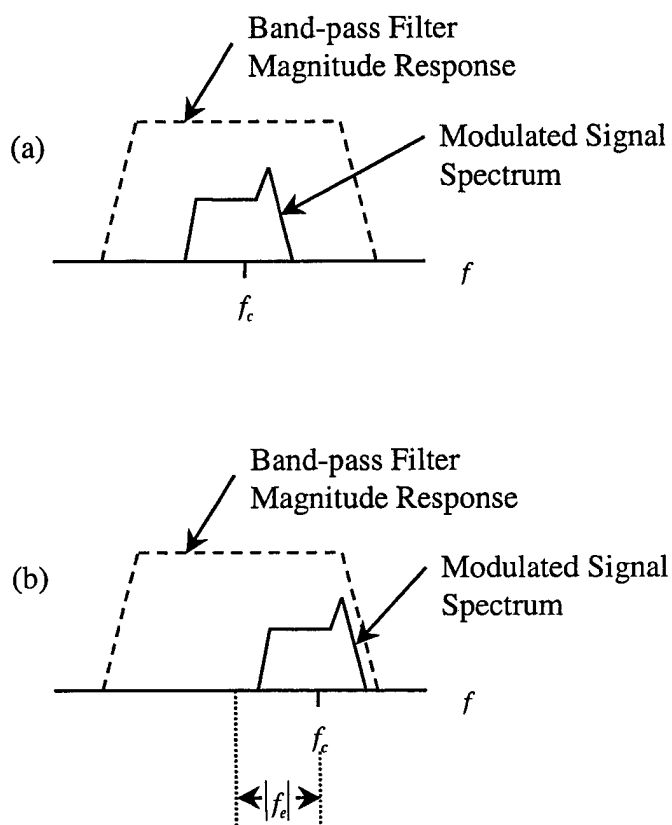


Figure 1-3. Representative Band-pass Filter processes; a) correct tuning frequency, b) tuning error offset.

### 1.1.3 Coherent Angle-Demodulation

A wealth of literature exists regarding the relatively complicated subject of coherent angle-demodulation. Therefore, only an overview of the basic concepts of this technique and the associated limitations and disadvantages will be presented. The advantage of the coherent angle-demodulation methods over those of the non-coherent methods is that the coherent methods utilize the a-priori knowledge that a signal has a large modulation index,  $\beta$  [2]. Coherent methods are therefore able to reject more of the additive noise,  $W_+(t)$ , while minimizing the rejection of the desired signal,  $s_+(t)$ .

Two specific coherent angle-demodulation methods are prevalent in the literature. These are the Phase Locked Loop (PLL) demodulator and the FM with Feedback (FMFB) demodulator. Which device performs better is a point of contention; however, Develet [3] has identified the PLL and FMFB devices to be “equivalent servo-mechanisms” under reasonable input signal and loop conditions. Develet’s view of the operation of these devices will be adopted for the purposes of this background, in the interest of brevity and clarity. Therefore, the FMFB demodulator will be presented as representative of the current methods of coherent angle-demodulation.

The FMFB demodulator is presented in Figure 1-4. Although low-pass filtering and integration are employed within the FMFB device itself, in general, further low-pass filtering and integration processes can be performed externally to the FMFB demodulator. The FMFB demodulator, therefore, replaces the Phase Differentiator of Figure 1-1. Under the condition that the time derivative of the angle of the unit-envelope prediction signal,  $\hat{s}_+^*(t)$ , closely follows the time derivative of the angle of the modulated constituent of input signal,  $X_+(t)$ , the complex multiplication

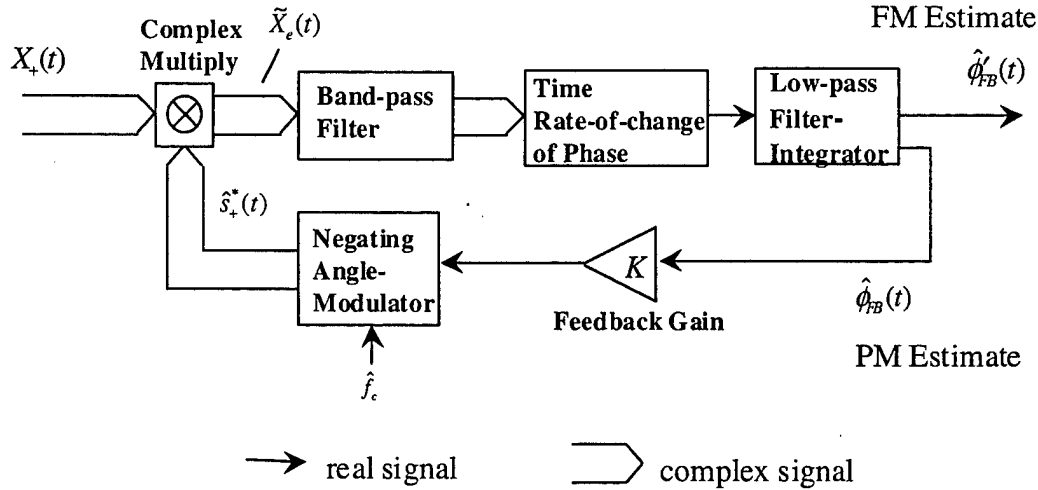


Figure 1-4. Analytic representation and implementation of the FMFB demodulator.

$$\tilde{X}_e(t) = X_+(t) \cdot \hat{s}_+^*(t) \quad (1.14)$$

will result in a reduced modulation index signal constituent. This message bearing constituent of the signal  $\tilde{X}_e(t)$ , can pass through a Band-pass Filter process, which is narrower than the Band-pass Filter processes depicted in Figure 1-1. Likewise, this Band-pass Filter process will pass less of the noise component,  $N_+(t)$ , when  $N_+(t)$  and  $s_+(t)$  are not highly correlated and  $s_+(t)$  is of sufficient strength. (As a practical matter, this Band-pass Filter process is implemented as a pair of identical real-valued low-pass filters, each operating on the real and imaginary components of  $\tilde{X}_e(t)$ . Thus the input and output of this filter are complex-valued, as shown in the figure.) Since the Band-pass Filter operates at a 0 Hz IF, both the input and output are considered to be complex envelope signals. As such, the Time Rate-of-change of Phase process shown in the



figure, can be implemented as previously described. Passing this result to the Low-pass Filter-Integrator results in the reduced modulation index frequency modulation estimate,  $\hat{\phi}'_{FB}(t)$ . Given that the goal is to reduce the modulation index at the output of the Band-pass Filter to the extent that is possible,  $\hat{\phi}'_{FB}(t)$  can be viewed as an error signal, which should approach some small level. By integrating this “error signal” to obtain  $\hat{\phi}_{FB}(t)$  and through use of the Feedback Gain,  $K$ , to control sensitivity, we have the ability to maintain a good quality prediction signal,  $\hat{s}_+^*(t)$ . The Negating Angle Modulator simply generates the unit-envelope prediction signal,

$$\hat{s}_+^*(t) = \exp\left\{-j \cdot \left[2\pi f_c t + K \hat{\phi}_{FB}(t)\right]\right\}, \quad (1.15)$$

which serves to reduce the modulation index of  $s_+(t)$ , as described. Thus negative feedback is employed through the phase of the prediction signal,  $\hat{s}_+^*(t)$ . With proper choice of Feedback Gain, Band-pass Filter and Low-pass Filter designs, the FMFB system will remain stable and reliably demodulate the input,  $X_+(t)$ .

#### 1.1.4 Limitations and Disadvantages of Coherent Angle-Demodulation

Both theory and practice verify that the FMFB and PLL demodulators reduce the distortion,  $\eta(t)$ , in large  $\beta$  systems. Specifically, these methods are found to reduce the FM threshold effect, where a rapid decrease in output signal-to-noise ratio (SNR) occurs for small decreases in input SNR. This threshold occurs at or about 10 dB input SNR.

Threshold improvements from 3 to 7 dB have been reported in the literature. Another advantage of the coherent method is that the adverse effects of a tuning error,  $f_e$ , can be mitigated. This is due to the fact that the coherent angle-demodulation process essentially tracks the center frequency,  $f_c$ , providing automatic tuning.

A disadvantage of the coherent angle-demodulation technique is that in many large  $\beta$  systems where threshold reduction is desired, a given combination of Feedback Gain, Band-pass Filter and Low-pass Filter processing may greatly reduce the noise, but at the same time cause excessive distortion of the original modulation. No mechanism is provided by the coherent angle-demodulator itself to compensate or correct for this distortion.

Another disadvantage of the coherent angle-demodulator is directly due to the fact that the modulation index is reduced. While this allows for the reduction of the additive noise,  $N(t)$ , there is a commensurate reduction in the recovered modulation signal strength. The result is that at input SNR values above threshold, coherent methods perform essentially the same as non-coherent methods of angle modulation recovery [4].

## 1.2 Standard Angle-Demodulation Results

To demonstrate the characteristics of the typical angle-demodulation process, simulation results are presented for the FM demodulation of a pulsed carrier, with imposed frequency modulation. A discrete-time implementation is used, with the commonly employed sample rate,  $F_s$ , of 2 Samples/Second. (This is an arbitrary but convenient choice of sample rate for simulations, leading to a Nyquist bandwidth of 1 Hz.) A backward difference FM demodulator [5] was used, with no explicit low-pass

post filtering. The imposed FM modulation is that of a linearly varying instantaneous frequency, from approximately  $-.08$  radians, to  $+.08$  radians. Additive White Gaussian Noise (AWGN) is combined with the pulsed carrier, at a 30 dB signal-to-noise ratio (SNR). Pulses were 200 samples in duration. A total of 100 pulses were generated, bandpass filtered, and demodulated, and the results averaged for comparison to the actual imposed FM modulation. The results are shown in Figure 1-5. The band-pass filter process was implemented in complex form, and used a finite impulse response (FIR) filter of 129 coefficients resulting from the Hanning windowed method of FIR filter design. A cutoff frequency of  $.25/4$  Hz is used.

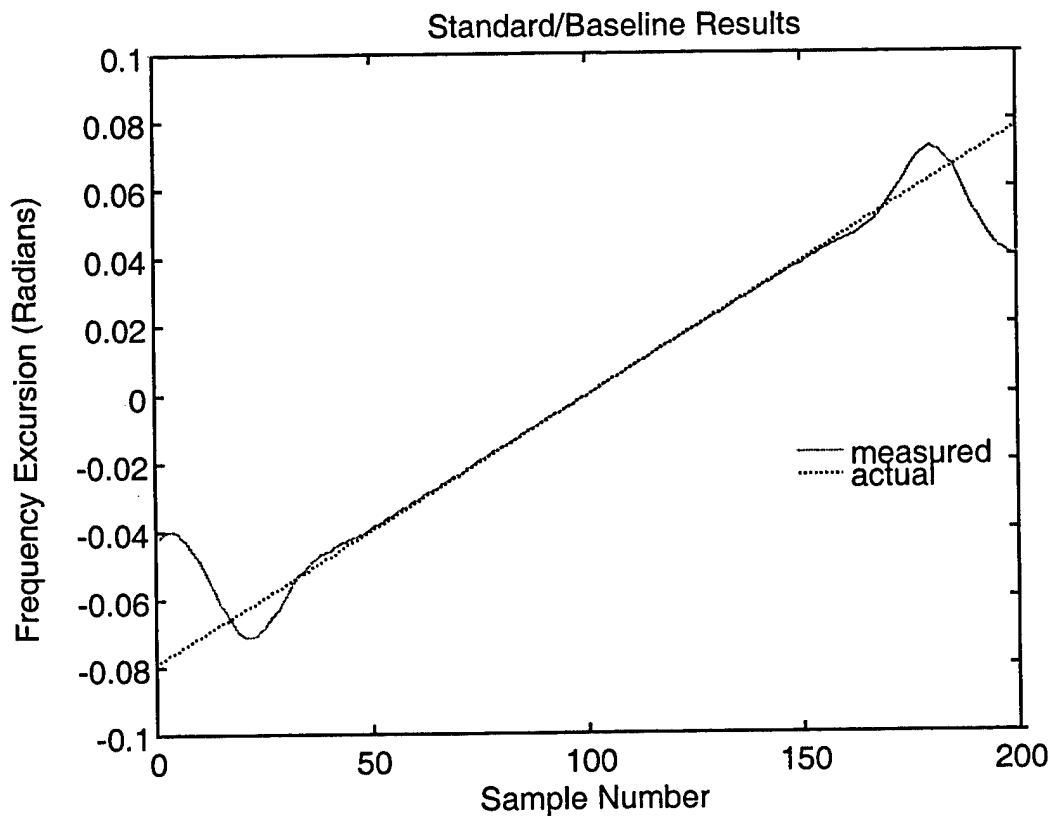


Figure 1-5. Recovered FM modulation as measured by a standard angle-demodulator.

The difference between the measured and actual FM modulation was also determined, and is shown in Figure 1-6. The corresponding root-mean-square (RMS) error was found to be .015182 radians.

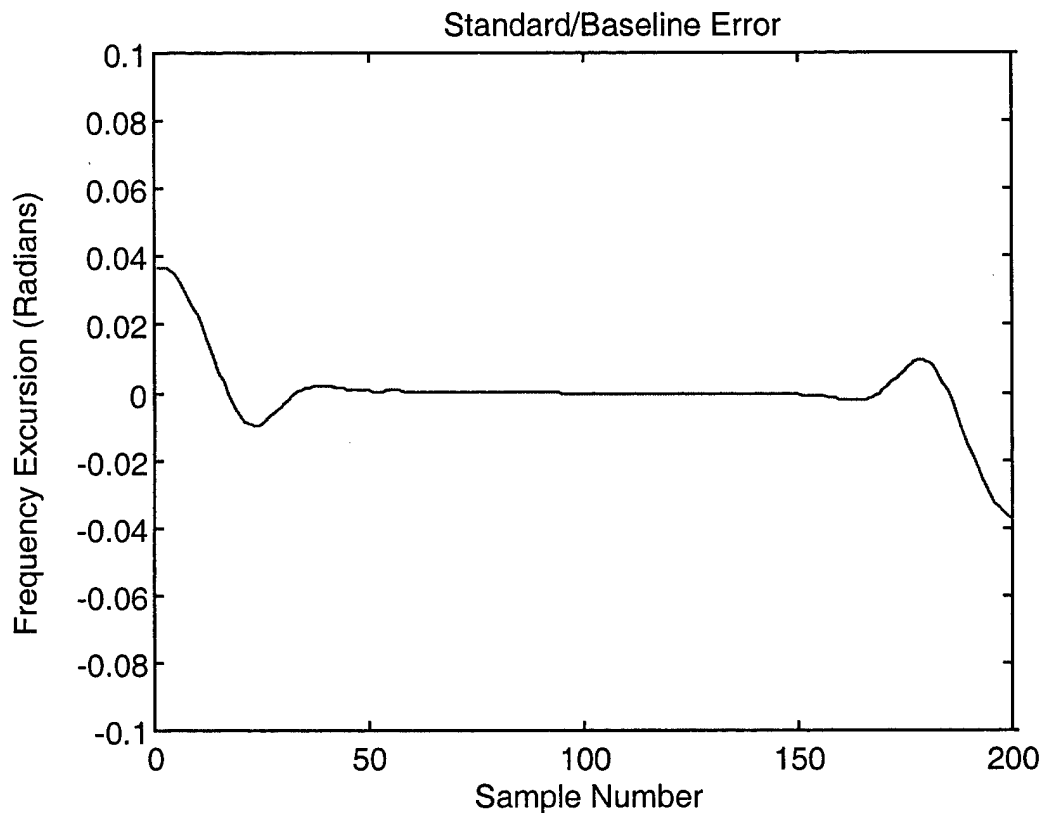


Figure 1-6. Recovered FM modulation measurement error resulting from a standard angle-demodulator.

## 2 RFF Background

In the course of further development of the Reconstituted FM with Feedback (R-FMFB or RFB) demodulator [6], it became apparent that we are not limited to the use of

feedback for enhancement of the modulation recovery process. In addition to feedback, feedforward mechanisms have been successfully employed in the development of system components such as amplifiers [7], to improve their linearity. As with these components it will be seen that signal delay becomes the enabling tool to effectively use feedforward concepts in angle modulation recovery.

## 2.1 Description, Manner and Process of Using the RFF Demodulator

A novel method of angle-demodulation, the RFF demodulator is presented in Figure 2-1. As seen in the figure, rather than feeding signals back to track the input, signals are fed forward from stage to stage, and within each stage. The input to this system is the complex envelope signal,  $\tilde{X}(t)$ , which contains both the desired signal constituent,  $\tilde{s}(t)$ , and the additive noise constituent,  $\tilde{N}(t)$ . Stages 2 through  $M$  of the RFF demodulator contain the same set of components, although different filter coefficients and Time Alignment Delay (TAD) processes may exist from stage to stage.

As shown in the figure, Stage 1 of the RFF demodulator is slightly different from the remaining stages, since the only necessary input to this stage is  $\tilde{X}(t)$ . The output of any particular stage,  $p$ , of the RFF demodulator consists of the complex envelope signals,  $\tilde{X}_p(t)$ , and  $\tilde{s}_p^*(t)$ , and the real FM estimate,  $\hat{\phi}'_p(t)$ . These outputs serve as inputs to stage  $p+1$ , for  $2 \leq p+1 \leq M$ . The phase modulation estimate,  $\hat{\phi}_M(t)$ , can optionally be output of Stage  $M$ , either in lieu of or in addition to  $\tilde{s}_M^*(t)$ , as an application requires. Note that the baseline or standard FM discriminator as described in previous sections, can be considered to be a 1-stage limiting form of the RFF demodulator.

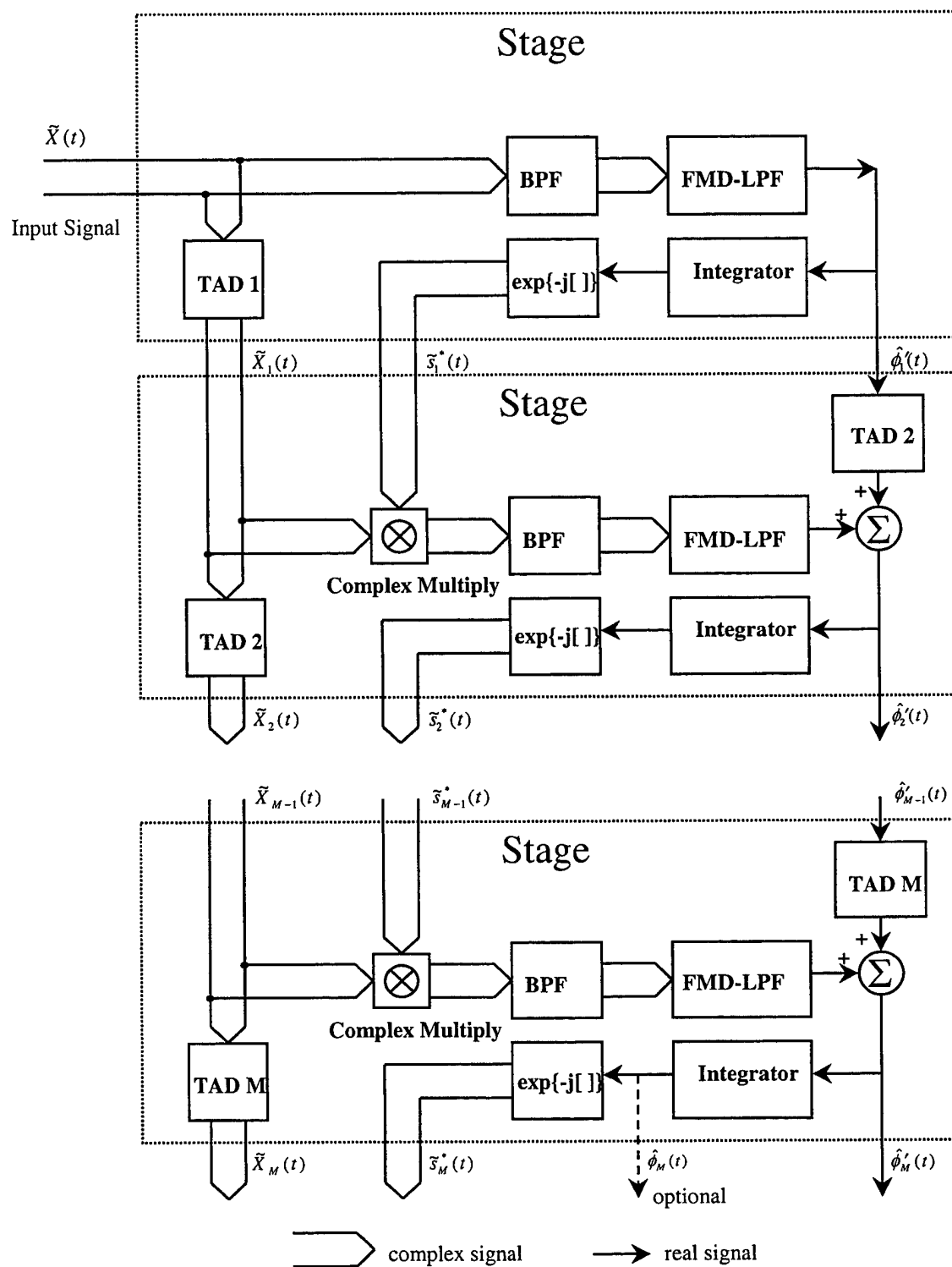


Figure 2-1. The RFF demodulator, U.S. Patent 6,002,298.

The goal of the RFF demodulator is the same as that of the FMFB demodulator, namely, to reduce the modulation index of the desired signal component,  $\tilde{s}(t)$ , and to employ a narrower band-pass filter process to pass this signal component while rejecting the noise component,  $\tilde{N}(t)$ . Referring to the figure, in a typical application each of the band-pass filters, BPF1 through BPFM, are designed to have a narrower bandwidth relative to the bandwidth of the zero-IF input signal,  $\tilde{X}(t)$ . As before, these band-pass filters are implemented as a pair of identical real low-pass filters operating on the real and imaginary components to be processed. The FM Demodulation-Low-pass Filtering process of each stage, FMD-LPF1 through FMD-LPFM, perform both time rate-of-change of phase measurement and low-pass filtering commensurate with the message signal bandwidth,  $f_m$ . The Time Alignment Delay processes, TAD1 through TADM, delay the real or complex signal inputs in time, by amounts equal to the time delay introduced by the BPF and the LPF processes of a particular stage. Thus for any particular stage,  $p$ , TAD $p$  provides a time delay equal to the sum of the time delays introduced by BPF $p$  and the low-pass filter portion of FMD-LPF $p$ . The Integrator processes shown in each stage invert the time rate-of-change of phase measurement (i.e., the FM demodulation process) for each stage. (For practical purposes, this integration process is often implemented in a modulo- $2\pi$  fashion.) Typically, the method of implementing the FMD portion of the FMD-LPF process would not change from stage to stage. This enhances the time alignment of the signals at summer node inputs in following stages. The  $\exp\{-j[\cdot]\}$  process of stage  $p$  simply negates the output of the

Integrator of the same stage prior to exponential modulation, resulting in the conjugate of the  $p^{th}$  desired modulated signal estimate,  $\tilde{s}_p^*(t)$ .

The output of any particular stage,  $p$ , therefore consists of the time aligned signals,  $\tilde{X}_p(t) = \tilde{X}_{p-1}(t - \tau_p)$ ,  $\tilde{s}_p(t) \equiv \tilde{s}_{p-1}(t - \tau_p)$  and  $\hat{\phi}'_p(t) \equiv \hat{\phi}'_{p-1}(t - \tau_p)$ , for  $2 \leq p \leq M$ . Here,  $\tau_p$  is the time delay amount that is introduced by the TAD $p$  process. These output signals serve as input to the stage proceeding. The time delay alignments thereby eliminate the need for feedback by using a feed-forward approach. The necessary modulation index reduction now takes place following Stage 1, in the Complex Multiply processes. Thus the Complex Multiply process of Stage 2 employs  $\tilde{s}_1(t)$ , an initial estimate of  $\tilde{s}(t)$ , to reduce the modulation index of  $\tilde{s}(t)$ . Once processed by BPF2 and FMD-LPF2, a reconstitution or recombination with  $\hat{\phi}'_1(t - \tau_2)$  replaces the modulation that was extracted by the Complex Multiply process, resulting in  $\hat{\phi}'_2(t)$ . This process of index reduction and reconstitution is repeated by each stage following. The RFF demodulator is therefore an iterative process which refines the output estimates,  $\tilde{s}_p^*(t)$  and  $\hat{\phi}'_p(t)$ . By appropriate design of BPF1 through BPFM and FMD-LPF1 through FMD-LPFM, the RFF demodulator enhances the angle-modulation recovery process in many modulation and additive interference scenarios where standard methods fail.

### 2.1.1 Alternative RFF Configurations

The Shannon/Nyquist sampling theorem of course applies to the RFF demodulator; both discrete-time (numerical) implementations and analog-time



implementations are conceivable. In particular, the discrete-time RFF demodulator can employ symmetric FIR filters with odd coefficient lengths, greatly simplifying TAD implementations and increasing accuracy.

Another alternative involves the use of a Reconstituted FM with Feedback [5, 6] or equivalent demodulator in stage 1. In large  $\beta$  scenarios, this modulation tracking device can cause the following stages of the RFF demodulator to converge more quickly and to a more accurate modulation estimate. This can also be a benefit in small  $\beta$  scenarios when the spectrum of  $m(t)$  contains significant energy at frequencies below  $f_m$  Hz.

### 2.1.2 RFF Advantages

The RFF demodulator provides the same benefits as the FMFB (or PLL) demodulator, while overcoming the previously cited disadvantages and limitations:

i) In the process of threshold enhancement by modulation index reduction and band-pass filtering, an excessive distortion of the original modulation can occur. This can happen as a result of setting the bandwidth of the band-pass filter to be more narrow than the bandwidth needed to process the reduced-index signal. The RFF demodulator provides a mechanism to compensate or correct for this distortion by iterative estimation refinement from stage to stage. This iterative estimation refinement results in a final modulation index reduction in Stage  $M$  such that BPFM is wide enough in bandwidth to pass the reduced-index signal, and narrow enough to provide an effective rejection of the additive noise,  $\tilde{N}(t)$ .

ii) An additional advantage of the RFF demodulator is due to the fact that modulation reconstitution occurs for each stage following stage 1. The result is that not only is the phase distortion term,  $\eta(t)$ , decreased, but this decrease is not at the expense of reducing the modulation term,  $\phi'(t)$ . Thus the device acts not only to minimize effects of additive noise, but also acts to maximize the recovered signal strength. Subsequently, at input SNR values above threshold, the RFF demodulator has the potential to out-perform previously described coherent and non-coherent methods of angle-modulation recovery, in many modulation scenarios.

iii) Another advantage is that for various input signal scenarios, where  $\beta$  is decreased, the RFF demodulator continues to provide threshold reduction, including scenarios where the modulated signal is considered to be narrow-band.

## 2.2 Demodulation Results Using the RFF

To demonstrate the characteristics of the RFF demodulator, a 5-stage RFF demodulator simulation has been implemented and tested against the same 100 pulsed carriers previously presented. This allows for direct comparison to the simulated baseline or standard angle-demodulation process. As before, the recovered pulse modulations were averaged together to represent the measured modulation. A backward difference FM demodulator was used in each stage, with no explicit low-pass filtering. The band-pass filter used in each stage was identical to that used in the simulated standard demodulator. The results are shown in Figures 2-2 and 2-3. Note the reduction in error over that of the standard demodulator results shown in Figures 1-5 and 1-6. In particular, the beginning and end of the recovered modulation is seen to have substantially less error. The

corresponding root-mean-square (RMS) error for the RFF measurement was found to be .004694 radians. This represents, for the example given, a 10.2 dB improvement over that of the baseline angle-demodulation results.

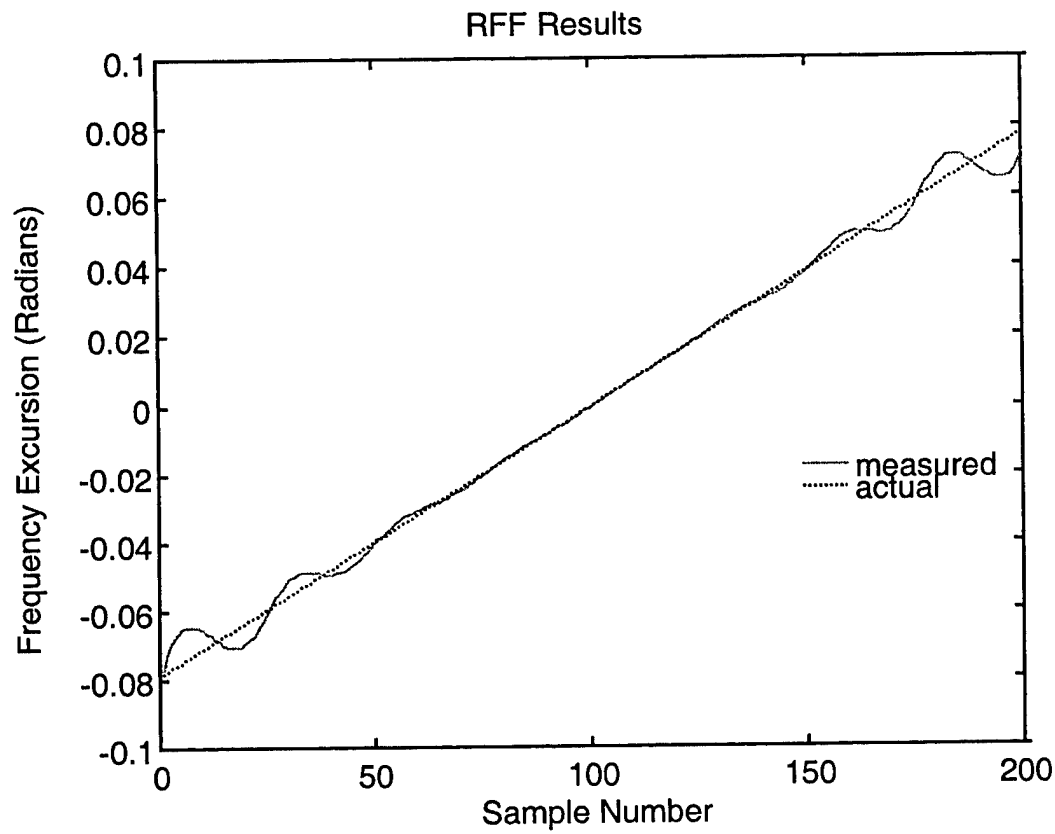


Figure 2-2. Recovered FM modulation as measured by an RFF demodulator.

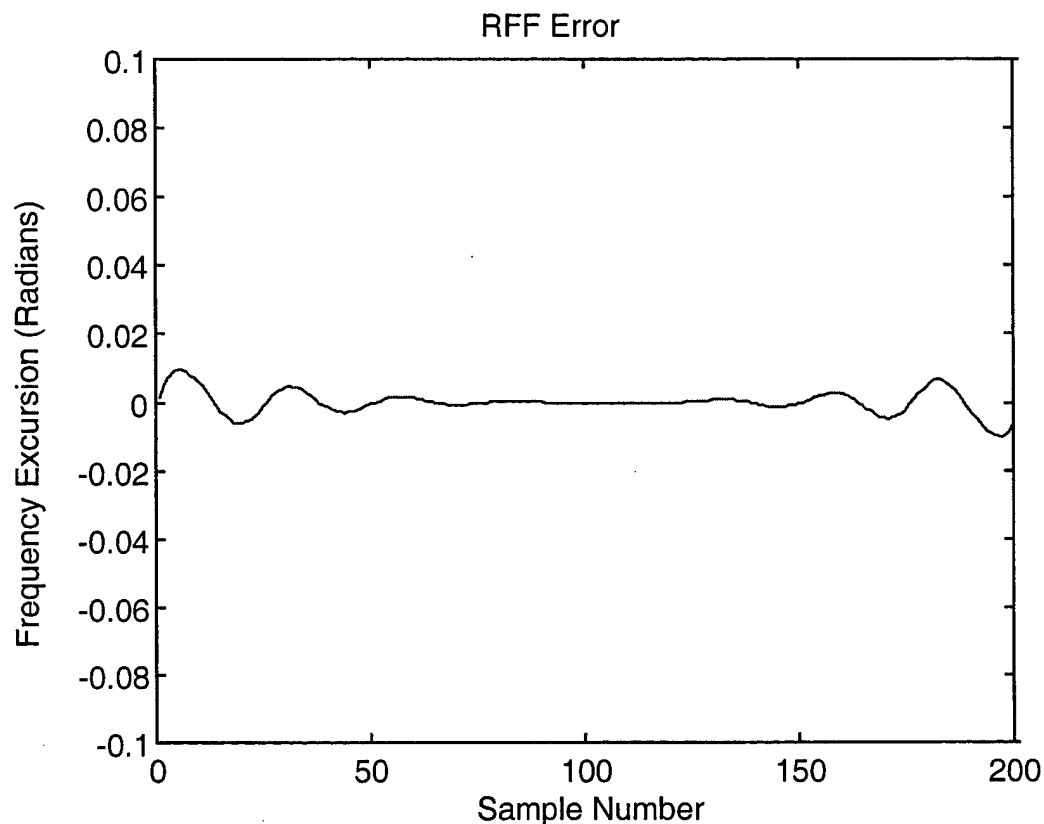


Figure 2-3. Recovered FM modulation measurement error resulting from an RFF demodulator.

### 3 Summary

This report has presented introductory material to motivate further research regarding the Reconstituted (Numerical) FM with Feedforward (RFF) demodulation technique. This introduction has included background in the areas of non-coherent and coherent angle-modulation recovery methods, along with their associated advantages and disadvantages. Based on this initial presentation of the RFF concept, further research can be performed, given the potential for increased recovered modulation fidelity.

Further areas of interest include experimental substantiation of the potential ability of the device to provide enhanced angle modulation recovery for various modulation formats, including Phase-Shift Keyed (PSK), Frequency Shift Keyed (FSK) and possibly Quadrature Amplitude Modulation (QAM) formats. In determining modulation formats that can best benefit from the RFF demodulator, it must also be determined where the RFF device is best applied within the recovery process. Candidate applications include signal-adaptive band-pass filtering, energy detection and synchronization.

#### 4 References

- [1] S. Haykin, *Communications Systems*, 2<sup>nd</sup> Ed., John Wiley & Sons, New York, 1983.
- [2] L. H. Enloe, "Decreasing the Threshold in FM by Frequency Feedback," *Proc, IRE*, vol. 50, pp. 18-30, January 1962.
- [3] J. A. Develet Jr., "Statistical Design and Performance of High-Sensitivity Frequency Feedback Receivers," *IEEE Trans. On Military Electronics*, pp. 281-284, October 1963.
- [4] M. Schwarz, W. R. Bennett, S. Stein, *Communications Systems and Techniques*, IEEE Press (Reprint), 1995.
- [5] A. J. Noga, "Numerical FM Demodulation Enhancements," Rome Laboratory Technical Report RL-TR-96-91, June 1996.
- [6] A. J. Noga, "Methods of Discrete-Time Phase and Frequency Synchronization," Air Force Research Laboratory Report AFRL-IF-RS-TR-1999-133, May 1999.
- [7] N. Potheary, *Feedforward Linear Power Amplifiers*, Artech House, 1999.

**MISSION  
OF  
AFRL/INFORMATION DIRECTORATE (IF)**

*The advancement and application of information systems science and technology for aerospace command and control and its transition to air, space, and ground systems to meet customer needs in the areas of Global Awareness, Dynamic Planning and Execution, and Global Information Exchange is the focus of this AFRL organization. The directorate's areas of investigation include a broad spectrum of information and fusion, communication, collaborative environment and modeling and simulation, defensive information warfare, and intelligent information systems technologies.*